

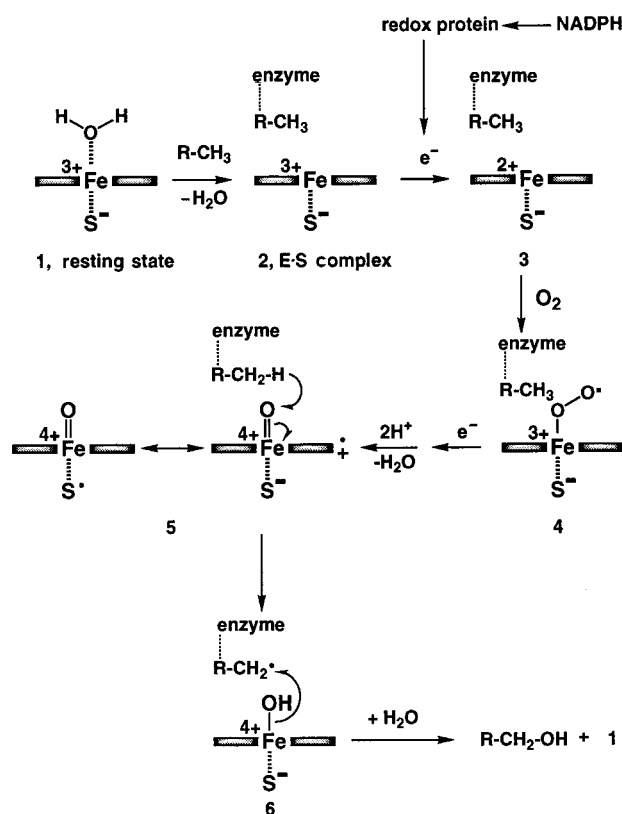
- [1] T. M. Kamenecka, S. J. Danishefsky, *Angew. Chem.* **1998**, *110*, 3164–3166; *Angew. Chem. Int. Ed.* **1998**, *37*, 2993–2995.
- [2] See inter alia a) W. E. Savage, *Aust. J. Chem.* **1975**, *28*, 2275; b) M. Nakagawa, S. Kato, S. Kataoka, S. Kodato, H. Watanabe, H. Okajima, T. Hino, B. Witkop, *Chem. Pharm. Bull.* **1981**, *29*, 1013; c) M. Somei, T. Kawasaki, Y. Fukui, F. Yamada, T. Kobayashi, H. Aoyama, D. Shinmyo, *Heterocycles* **1992**, *34*, 1877.
- [3] Prepared from *L*-*N*<sub>5</sub>-trityltryptophan and *N,N'*-diisopropyl-*O*-*tert*-butylisourea (CH<sub>2</sub>Cl<sub>2</sub>, RT): P. A. Hipskind, J. J. Howbert, S. Cho, J. S. Cronin, S. L. Fort, F. O. Ginah, G. J. Hansen, B. E. Huff, K. L. Lobb, M. J. Martinelli, A. R. Murray, J. A. Nixon, M. A. Staszak, J. D. Copp, *J. Org. Chem.* **1995**, *60*, 7033.
- [4] D. Evans, T. C. Britton, R. L. Dorow, J. F. Dellaria, *J. Am. Chem. Soc.* **1986**, *108*, 6395.
- [5] Compound **12** was more conveniently prepared in bulk by a non-stereospecific route starting with (*R*)-methyl 4,5-epoxypentanoate: P. T. Ho, N. Davies, *Synthesis* **1983**, 462.
- [6] O. Kitagawa, T. Sato, T. Taguchi, *Chem. Lett.* **1991**, 177.
- [7] J. M. Humphrey, A. R. Chamberlin, *Chem. Rev.* **1997**, *97*, 2243.

## On the Origin of the Low-Spin Character of Cytochrome P450<sub>cam</sub> in the Resting State—Investigations of Enzyme Models with Pulse EPR and ENDOR Spectroscopy\*\*

Hamed Aissaoui, Rainer Bachmann,  
Arthur Schweiger, and Wolf-Dietrich Woggon\*

The cytochrome P450 enzymes, ubiquitous in nature, are heme–thiolate proteins which are important to the metabolism of endogenous compounds and xenobiotics.<sup>[1]</sup> The reactivity of these enzymes is associated with an iron(III)–protoporphyrin IX complex in the active site which is bound to the protein through hydrogen bridges of the two propionate side chains and through a thiolate ligand provided by a cysteine residue; the thiolate ligand is coordinated to the iron center from the proximal side of the porphyrin.

Our knowledge of various intermediates in the catalytic cycle of cytochromes P450 (Scheme 1) relies on X-ray structures of different forms of cytochrome P450<sub>cam</sub><sup>[2, 3]</sup> and numerous investigations on suitable model compounds.<sup>[4]</sup> Accordingly, the resting state of cytochrome P450<sub>cam</sub> (**1**) contains six water molecules in the substrate binding domain (one water molecule is coordinated to the iron center) which are all displaced when the natural substrate camphor is bound. It was recently suggested that Arg299, which according to the X-ray structure forms a salt bridge with one of the heme propionate



Scheme 1. Catalytic cycle of cytochrome P450.

groups, triggers the release of the active-site water cluster through a pathway other than the substrate access channel. On substrate binding, conformational changes of the propionate/Arg299 domain open a channel to a water cluster located close to the protein surface, on the proximal side of the heme.<sup>[5]</sup>

This change in the ligand sphere of iron is accompanied by a change in the spin-state equilibrium from greater than 96 % low-spin Fe<sup>III</sup> in the resting state **1** to predominantly high-spin Fe<sup>III</sup> of the E·S complex **2**.<sup>[6]</sup> The redox potential of the heme–thiolate protein also shifts from –300 mV for **1** to –175 mV for **2**, rendering the latter capable of accepting an electron from NADPH through the redox protein putida-redoxin. Subsequently, the iron(II) complex **3** is formed, which binds oxygen to yield **4**. Reductive scission of the oxygen–oxygen bond furnishes the iron(IV) oxo intermediate **5**, which allows, for example, O insertion into nonactivated C–H bonds (see **6**).<sup>[4]</sup> Whether O insertion is in general a two-step process, as shown in Scheme 1, or whether it can also proceed in a concerted fashion is currently being disputed.<sup>[7]</sup>

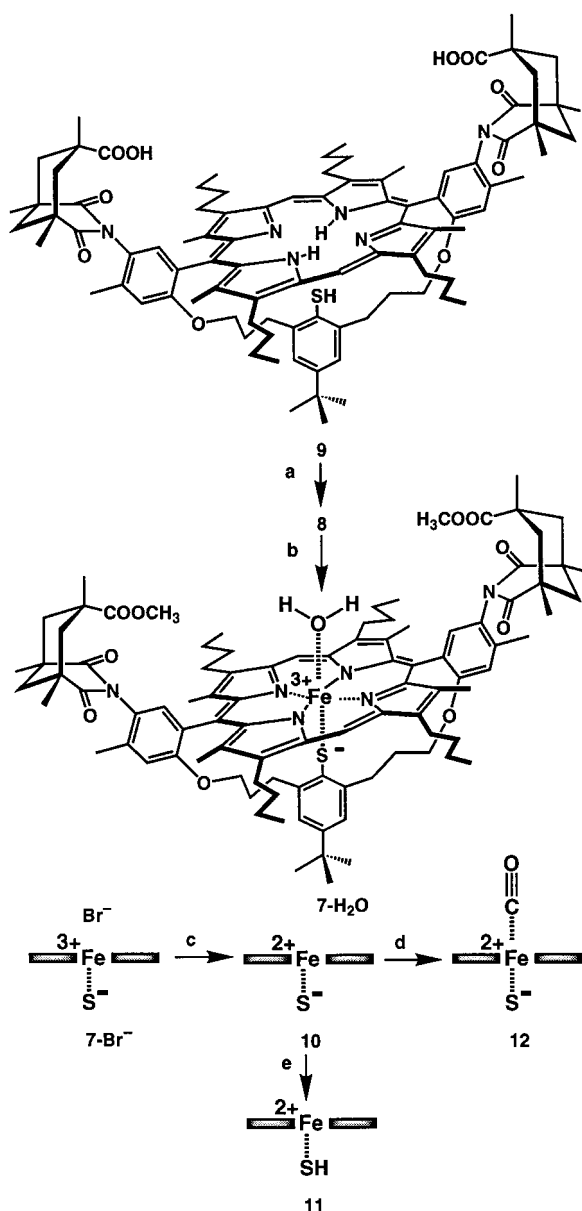
Ever since the water cluster was discovered in **1**, the origin of the low-spin ground state has been a matter of debate, as it seems unlikely that thiolate and water, both weak ligands, would establish a low-spin iron(III) center. It was therefore suggested that –OH rather than water binds to iron or that the hydrogen-bonded water cluster induces a hydroxide-like character at the coordinated water molecule.<sup>[2b, 8]</sup> From ESEEM studies (ESEEM = electron spin echo envelope modulation) with <sup>17</sup>O-enriched water bound to P450<sub>cam</sub>, however, it was concluded that one water molecule binds

[\*] Prof. Dr. W.-D. Woggon, Dipl.-Chem. H. Aissaoui  
Institut für Organische Chemie der Universität  
St.-Johanns-Ring 19, CH-4056 Basel (Switzerland)  
Fax: (+41) 61-267-11-02  
E-mail: woggon@wolfe.chemie.unibas.ch  
Dr. R. Bachmann, Prof. Dr. A. Schweiger  
Laboratorium für Physikalische Chemie  
Eidgenössische Technische Hochschule  
CH-8092 Zürich (Switzerland)

[\*\*] This research was supported by the Swiss National Science Foundation. Gunnar Jeschke is gratefully acknowledged for stimulating discussions.

nonrandomly to iron; the presence of a hydroxide ion as the sixth ligand was excluded.<sup>[9]</sup> Since these investigations arrived at no conclusions whatsoever concerning the origin of the low-spin character of iron(III) in the given ligand field, we decided to prepare suitable enzyme models for the resting state of P450<sub>cam</sub> to investigate these complexes by CW EPR as well as pulse EPR and ENDOR techniques (CW = continuous wave, EPR = electron paramagnetic resonance, ENDOR = electron nuclear double resonance). Such studies should provide information on the possible structure and electronic nature of the first intermediate in the catalytic cycle of cytochrome P450<sub>cam</sub>.

The P450 analogue **7** was prepared via **8** from the diacid **9**, a recently synthesized ligand for a P450 model with substrate recognition sites (Scheme 2).<sup>[10]</sup> After insertion of the iron



Scheme 2. Synthesis of **7-H<sub>2</sub>O**, a spectroscopic and chemical enzyme model for the resting state of cytochrome P450<sub>cam</sub>: a) CH<sub>2</sub>N<sub>2</sub>, CH<sub>2</sub>Cl<sub>2</sub>, 25 °C, 30 min; b) FeBr<sub>2</sub>, 2,6-lutidine, toluene, reflux, 1 h; c) KH, [18]crown-6, benzene, 25 °C, 30 min; d) CO, toluene, 25 °C, 30 min; e) silica gel, [D<sub>8</sub>]toluene.

center, the bromide **7-Br<sup>-</sup>** was isolated ( $\lambda_{\text{max}} = 400$  nm). Reduction of **7-Br<sup>-</sup>** with KH in benzene/[18]crown-6 yielded the iron(II) complex **10** ( $\lambda_{\text{max}} = 422$  nm), which was spectroscopically characterized in its protonated form **11**. Complex **10** binds CO to give **12**, which exhibits a shifted Soret band at 448 nm, characteristic of cytochrome P450. Furthermore, in catalytic amounts, **7** performs reactions common to P450 enzymes in the presence of "O" donors.<sup>[11]</sup> When **7-Br<sup>-</sup>** was treated with water/toluene for 24 h the iron(III)–porphyrin **7-H<sub>2</sub>O** was obtained; it was characterized by a Soret band at 408 nm. Electron spray ionization (ESI) mass spectrometry ( $m/z$ : 1623 [ $M^+$ ]) indicated the coordination of one molecule of water to the iron center from the distal side. Accordingly, complex **7** qualifies as a good spectroscopic and chemical enzyme model for the resting state of cytochrome P450.

In native P450<sub>cam</sub> the change from the state with hexacoordinated low-spin Fe<sup>III</sup> in **1** to the state with pentacoordinated high-spin Fe<sup>III</sup> in the enzyme–substrate complex **2** can be easily monitored by CW EPR spectroscopy. The low-spin state **1** shows an EPR spectrum with  $g$  values at 2.45, 2.26, and 1.91. The addition of camphor results in a conversion into a rhombically distorted high-spin form **2** with  $g = 7.85$ , 3.97, and 1.78.<sup>[12, 13]</sup> Figure 1a displays the CW EPR spectrum of the

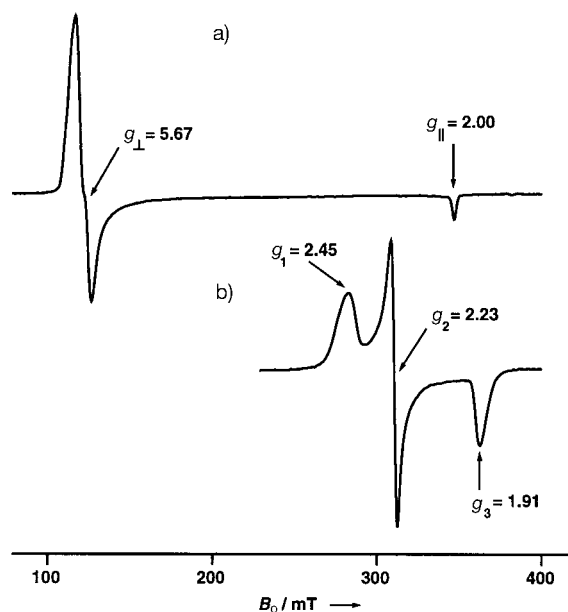
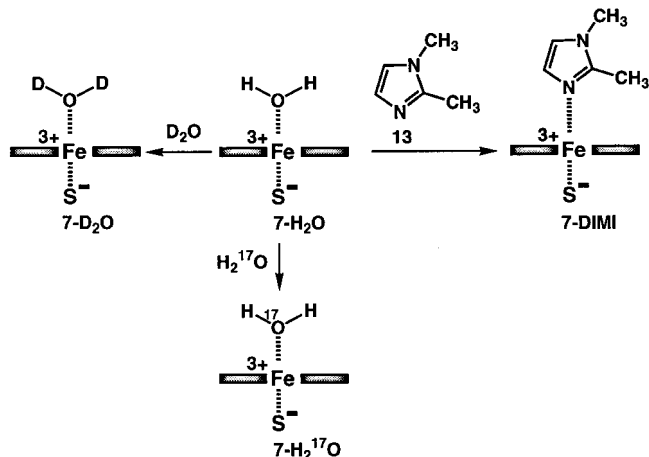


Figure 1. a) CW EPR spectrum of the high-spin state of **7-H<sub>2</sub>O** (solvent: MTHF;  $T = 10$  K). b) CW EPR spectrum of the low-spin state **7-DIMI** (solvent: MTHF;  $T = 100$  K).

synthetic P450 analogue **7-H<sub>2</sub>O** at 10 K. The almost axially symmetric EPR spectrum with  $g_{\perp} = 5.67$  and  $g_{\parallel} = 2.00$  is characteristic of high-spin iron(III) porphyrins without significant rhombic contributions from the ligand field. It is established that the  $g_{\parallel}$  extremum is normal to the porphyrin plane and that of  $g_{\perp}$  lies in the porphyrin plane.<sup>[14]</sup> Since the only indication of coordination of water to the iron center in **7-H<sub>2</sub>O** came from the ESI mass spectrum, a more complete characterization of the iron(III) ligand sphere by pulse EPR and ENDOR techniques was required.

Replacement of the water ligand in **7**-H<sub>2</sub>O by treatment with an excess of 1,2-dimethylimidazole (DIMI, **13**) induced a change to the low-spin complex **7**-DIMI (Scheme 3). It is important to note that the corresponding CW EPR spectrum



Scheme 3. Exchange reactions of the distal, sixth ligand of **7**-H<sub>2</sub>O.

(Figure 1b) shows *g* values (2.45, 2.23, and 1.91) almost identical to those of the native P450<sub>cam</sub> in its low-spin state **1**. This additional spectroscopical conformity between the enzyme's resting state and its model system **7** lends further evidence to the suitability of the latter as an active-site analogue.

Concerning the coordination of water to Fe<sup>III</sup>, the proton hyperfine couplings of several comparable native high- and low-spin heme systems are known from ENDOR studies.<sup>[15]</sup> In the high-spin case the expected proton hyperfine coupling along *g*<sub>||</sub> (*a*<sub>iso</sub> + *A*(*g*<sub>||</sub>)) lies around 6 MHz and is predominantly dipolar in character.<sup>[16]</sup> The three-pulse ESEEM spectrum of **7**-H<sub>2</sub>O shows no evidence of such a strong proton interaction (Figure 2a). Stirring **7**-H<sub>2</sub>O in a mixture of 2-methyltetrahydrofuran (MTHF) and D<sub>2</sub>O for 12 h provided the corresponding deuterated complex **7**-D<sub>2</sub>O; its three-pulse ESEEM spectrum reveals an intensive deuterium signal pair centered at the nuclear Zeeman frequency of deuterium with a splitting of 1.04 MHz (Figure 2b).

The Fourier transformation of the ratio of the time domain signals of **7**-D<sub>2</sub>O/**7**-H<sub>2</sub>O includes only the deuterium modulation (Figure 2c), although, in principle, residual lines at frequencies corresponding to other nuclei and their combinations should be present. The intensities of these are, however, very small and can be neglected.<sup>[9a, 17]</sup>

From the deuterium interaction the expected proton coupling normal to the porphyrin plane can be calculated to 6.77 MHz (*g*<sub>H</sub>/*g*<sub>D</sub> = 6.51). A proton hyperfine coupling of exactly this value can be detected in the Davies ENDOR spectrum of **7**-H<sub>2</sub>O (Figure 3a). The corresponding signal pair can be completely removed by exchange with D<sub>2</sub>O; in contrast, all the other proton lines are not affected by the exchange reaction (Figure 3b).

In the Davies ENDOR spectrum the deuterium coupling is not detectable since this technique is not sensitive enough at low frequencies. On the other hand, the broad proton lines

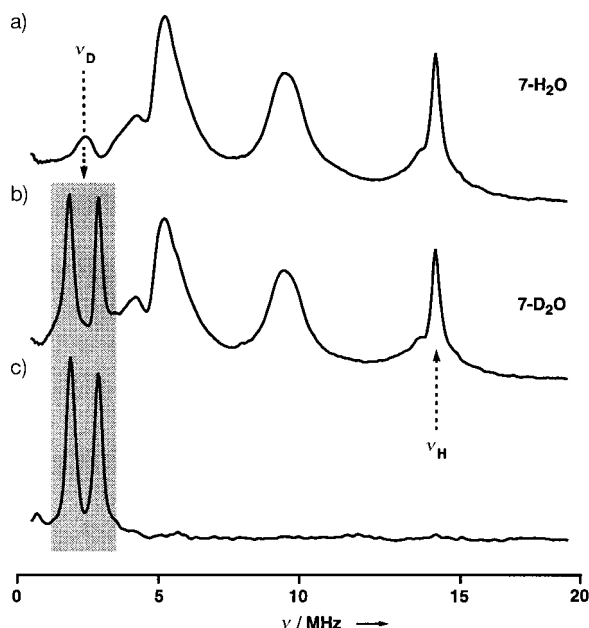


Figure 2. a), b) Three-pulse ESEEM spectra of **7**-H<sub>2</sub>O and **7**-D<sub>2</sub>O (solvent: MTHF; *T* = 3.3 K; orientation: *g*<sub>||</sub>; summation of 64 *τ* values. c) Fourier transform of the ratio of the time traces of **7**-H<sub>2</sub>O and **7**-D<sub>2</sub>O.

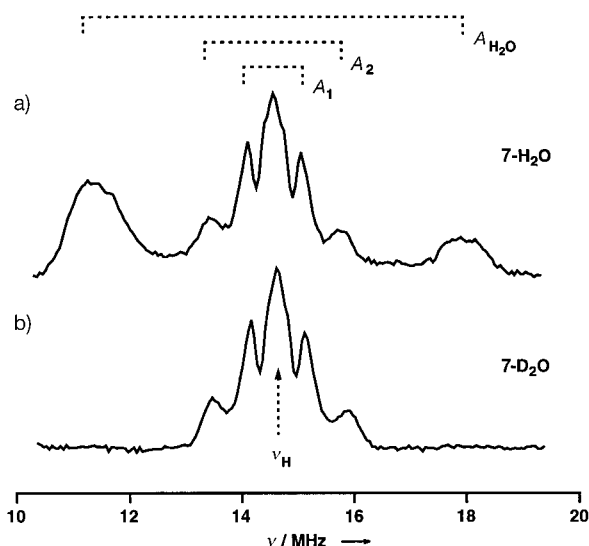


Figure 3. Davies ENDOR spectrum (proton region) of a) **7**-H<sub>2</sub>O and b) **7**-D<sub>2</sub>O (solvent: MTHF; *T* = 3.3 K; orientation: *g*<sub>||</sub>).

cannot be seen in the three-pulse ESEEM due to spectrometer dead time. Thus, Davies ENDOR and three-pulse ESEEM spectroscopy complement each other in an optimal fashion. The well-resolved small proton hyperfine couplings *A*<sub>1</sub> = 0.95 MHz and *A*<sub>2</sub> = 2.30 MHz (Figure 3) can tentatively be assigned to the *meso* protons of the porphyrin ligand and to the benzylic protons of the thiophenolate bridge spanning the porphyrin, respectively.

In further experiments the H<sub>2</sub>O ligand of **7**-H<sub>2</sub>O was exchanged for H<sub>2</sub><sup>17</sup>O. The resulting complex **7**-H<sub>2</sub><sup>17</sup>O shows no line broadening in the CW EPR spectrum; the Davies ENDOR spectrum, however, is very informative (Figure 4). Subtraction of the ENDOR spectra of **7**-H<sub>2</sub><sup>17</sup>O and **7**-H<sub>2</sub>O

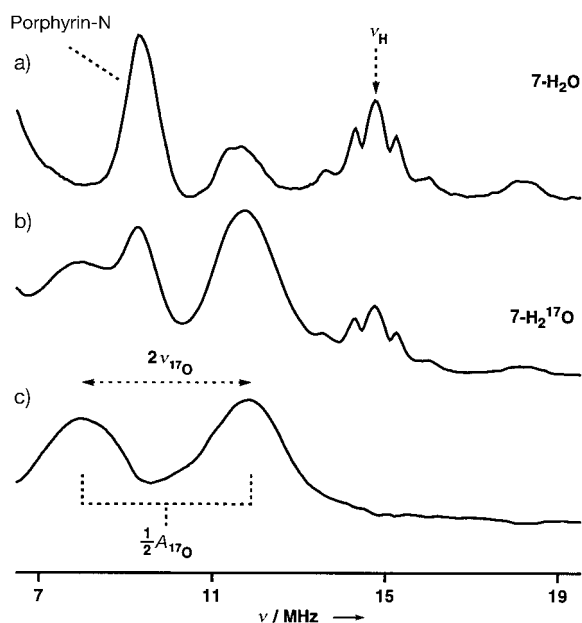


Figure 4. a), b) Davies ENDOR spectra of  $7\text{-H}_2\text{O}$  and  $7\text{-H}_2^{17}\text{O}$  (not to scale; solvent: MTHF;  $T = 3.3\text{ K}$ ; orientation:  $g_{\parallel}$ ). c) Subtraction of the spectrum of  $7\text{-H}_2\text{O}$  from the spectrum of  $7\text{-H}_2^{17}\text{O}$ .

reveals two intense  $^{17}\text{O}$  lines centered at  $1/2 A(^{17}\text{O})$  ( $A(^{17}\text{O}) = 19.83\text{ MHz}$ ); the splitting of the two signals corresponds to twice the nuclear Zeeman frequency of  $^{17}\text{O}$  ( $2\nu(^{17}\text{O}) = 3.98\text{ MHz}$ ), and the broadening is due to the nuclear quadrupole interaction of  $^{17}\text{O}$  ( $I = 5/2$ ). This hyperfine coupling is remarkably strong in comparison to the very weak  $\text{Fe}-^{17}\text{O}$  interaction in the low-spin state **1**, where the unpaired electron resides predominantly in the  $d_{yz}$  orbital of  $\text{Fe}^{\text{III}}$ .<sup>[9a]</sup>

Accordingly, it is unequivocally demonstrated that  $7\text{-H}_2\text{O}$  is a hexacoordinated iron(III) porphyrin in which a thiolate ligand and a water molecule coordinate to the iron center. In contrast to **1**, the resting state of  $\text{P450}_{\text{cam}}$ , the synthetic analogue  $7\text{-H}_2\text{O}$  is definitely in the high-spin state and changes only to a low-spin system if the water ligand is exchanged for a strong ligand, such as 1,2-dimethylimidazole (**13**). In view of the ESEEM studies of the enzyme  $\text{P450}_{\text{cam}}$  discussed above,<sup>[9]</sup> water rather than a stronger ligand such as a hydroxide ion coordinates to the iron(III) center. Consequently, the coordination of water to iron in the active site of cytochrome P450 is not the single determining factor for establishing the low-spin character of the system. The results presented here provide the first experimental support for calculations reported recently.<sup>[18]</sup> The INDO/ROHF and molecular dynamics simulations of cytochrome  $\text{P450}_{\text{cam}}$  suggested two cooperative factors favoring the low-spin state of **1**: The coordination of the water ligand to iron decreases the energy difference between the high-spin and low-spin states from  $75.4$  to  $15.9\text{ kJ mol}^{-1}$ , and the electrostatic field from the protein can further stabilize the low-spin state by  $7.5\text{ kJ mol}^{-1}$  below the high-spin state.

Regarding our enzyme model, a simple estimation revealed that a point charge  $7\text{ \AA}$  above the porphyrin plane of  $7\text{-H}_2\text{O}$  would be sufficient to establish an electrostatic potential of about  $2\text{ V}$ . According to the calculations,<sup>[18]</sup> this would be

enough to decrease the energy of the low-spin state of  $\text{P450}_{\text{cam}}$  significantly below that of the high-spin state. Work is in progress to mimic the significance of the protein's electric field through attachment of positively charged substituents to the Kemp acids of  $7\text{-H}_2\text{O}$ .<sup>[19]</sup>

### Experimental Section

**8:** To a solution of porphyrin **9**<sup>[10]</sup> (60 mg, 0.04 mmol) in  $\text{CH}_2\text{Cl}_2$  (10 mL) was added dropwise a  $0.23\text{ M}$  solution of  $\text{CH}_2\text{N}_2$  (3 mL) in ether. The red solution was stirred for 30 min under argon at  $25^\circ\text{C}$ . After evaporation of the solvent in vacuo the residue was purified by flash chromatography on silica gel (toluene/AcOEt 8/2) to give 52 mg (0.033 mmol, 83 %) of **8** as a red solid. TLC (toluene/AcOEt 8/2):  $R_f = 0.85$ ; m.p.  $> 250^\circ\text{C}$ . UV/Vis ( $\text{CH}_2\text{Cl}_2$ ):  $\lambda_{\text{max}}$  (%) = 416 (100), 510 (12), 574 (8), 588 (5), 654 nm (3);  $^1\text{H}$  NMR (300 MHz,  $[\text{D}_6]\text{acetone}$ ):  $\delta = 10.15$  (s, 2H, meso-H), 8.35 (s, 2H, Ar-H), 7.17 (s, 2H, Ar-H), 6.26 (s, 2H, Ar-H), 4.05–4.01 (m, 8H, pyrrole- $\text{CH}_2$ ), 3.71–3.69 (m, 4H,  $\text{OCH}_2$ ), 3.35 (s, 6H,  $\text{COOMe}$ ), 2.80–2.77 (s, 12H, pyrrole- $\text{CH}_3$  and m, 4H,  $\text{H}_{\text{eq}}$ ), 2.39 (d,  $J = 13.02\text{ Hz}$ , 2H,  $\text{H}_{\text{eq}}$ ), 2.30 (s, 6H, Ar- $\text{CH}_3$ ), 2.17–2.13 (m, 8H, pyrrole- $\text{CH}_2\text{CH}_2$ ), 1.82–1.77 (m, 8H, pyrrole- $(\text{CH}_2)_2\text{CH}_2$ ), 1.43 (s, 16H, 4Me), 1.29 (s, 6H, 2Me), 1.16 (m, 6H,  $\text{H}_{\text{ax}}$ ), 1.09 (t, 12H, pyrrole- $(\text{CH}_2)_2\text{CH}_2$ ), 0.86 (s, 9H,  $t\text{Bu}$ ), 0.85 (m, 4H,  $\text{OCH}_2\text{CH}_2$ ), 0.62–0.50 (m, 4H,  $\text{O}(\text{CH}_2)_2\text{CH}_2$ ),  $-2.10$  (s, 1H, NH),  $-2.65$  (s, 1H, NH),  $-3.10$  (s, 1H, SH); ESI-MS ( $\text{CH}_2\text{Cl}_2/\text{MeOH}$  1/9):  $m/z$ : 1552 [ $M^+$ ]; MALDI-TOF:  $m/z$ : 1551 [ $M^+$ ] ( $\text{C}_{96}\text{H}_{122}\text{N}_6\text{O}_{10}\text{S}$  (1550.89)).

**7-Br $^-$ :** In a glove box, three drops of 2,6-lutidine and a spatula of  $\text{FeBr}_2$  were added to a solution of **8** (50 mg, 0.032 mmol) in refluxing toluene (10 mL). The dark brown solution was stirred at reflux for 1 h. After evaporation of the solvent the residue was purified by flash chromatography on silica gel (toluene/AcOEt 8/2) to give 39 mg (0.024 mmol, 76 %) of **7-Br $^-$**  as a brown solid. TLC (toluene/AcOEt 8/2):  $R_f = 0.75$ ; m.p.  $> 250^\circ\text{C}$ ; UV/Vis (toluene):  $\lambda_{\text{max}}$  (%) = 400 (100), 512 (8), 592 nm (5);  $^1\text{H}$  NMR (250 MHz,  $\text{CDCl}_3$ ): 78.9 (brs, 2H, meso-H), 40.5 (s, 12H, pyrrole- $\text{CH}_3$ ), 38.5 (s, 8H, pyrrole- $\text{CH}_2$ ), 12.8 (s, 2H, Ar-H), 9.5 (m, 4H, Ar-H), 5.3 (s, 6H,  $\text{COOMe}$ ), 4.96 (m, 6H,  $\text{OCH}_2$ , 4H $_{\text{eq}}$ ), 3.84 (m, 6H,  $\text{OCH}_2\text{CH}_2$ , 4H $_{\text{ax}}$ ), 3.23 (s, 6H, Ar- $\text{CH}_3$ ), 2.99 (m, 8H, 2H $_{\text{ax}}$  + 2H $_{\text{eq}}$ , pyrrole- $\text{CH}_2\text{CH}_2$ ), 2.69 (m, 8H, pyrrole- $(\text{CH}_2)_2\text{CH}_2$ ), 2.45 (s, 6H, 2Me), 1.77 (s, 12H, 4Me), 1.3 (m, 12H, pyrrole- $(\text{CH}_2)_3\text{CH}_3$ ), 0.91 (s, 9H,  $t\text{Bu}$ ), 0.11 (s, 4H,  $\text{O}(\text{CH}_2)_2\text{CH}_2$ ); ESI-MS ( $\text{CH}_2\text{Cl}_2/\text{MeOH}$  1/9):  $m/z$ : 1606 [ $M^+$ ]; MALDI-TOF:  $m/z$ : 1606 [ $M^+$ ] ( $\text{C}_{96}\text{H}_{119}\text{N}_6\text{O}_{10}\text{FeS}$  (1603.81)); both MS techniques display  $M^+$  devoid of the  $\text{Br}^-$  counterion.

**7-H $_2\text{O}$ :** To a solution of **7-Br $^-$**  (10 mg, 6.23  $\mu\text{mol}$ ) in toluene (2 mL) was added water (0.5 mL). The mixture was stirred for 20 h at  $25^\circ\text{C}$  under argon. The organic phase was separated and concentrated in vacuo to give a crude brown solid. Flash chromatography on silica gel (toluene/AcOEt 8/2) gave 7 mg (4.32  $\mu\text{mol}$ , 69 %) of **7-H $_2\text{O}$**  as a brown solid. UV/Vis ( $\text{CH}_2\text{Cl}_2$ ):  $\lambda_{\text{max}}$  (%) = 408 (100), 519 (7), 595 nm (3); ESI-MS ( $\text{CH}_2\text{Cl}_2/\text{MeOH}$  1/9):  $m/z$ : 1623 [ $M^+$ ] ( $\text{C}_{96}\text{H}_{121}\text{N}_6\text{O}_{11}\text{FeS}$  (1621.82)).

**10 and 11:** In a glove box one small spatula of potassium hydride and three crystals of [18]crown-6 were added to a solution of **7-Br $^-$**  (10 mg, 6.23  $\mu\text{mol}$ ) in  $[\text{D}_6]\text{benzene}$  (0.2 mL). The red solution was stirred at  $25^\circ\text{C}$  for 30 min, and a small sample was removed to confirm the formation of **10**; UV/Vis (toluene):  $\lambda_{\text{max}}$  (%) = 422 (100), 565 (8), 655 nm (5). The mixture was then purified by flash chromatography on silica gel ( $[\text{D}_8]\text{toluene}$ ) to give **11** as a red solid; UV/Vis (toluene):  $\lambda_{\text{max}}$  (%) = 418 (100), 486 (13), 510 (9), 564 (5), 622 (3), 648 nm (2);  $^1\text{H}$  NMR (250 MHz,  $[\text{D}_8]\text{toluene}$ ):  $\delta = 39.96$  (s, 2H, meso-H), 7.1 (s, 4H, Ar-H), 6.96 (s, 2H, Ar-H), 4.50 (m, pyrrole- $\text{CH}_2$ ), 4.28 (m, 4H,  $\text{OCH}_2$ ), 3.9–2.5 (m, 32H), 2.38 (s, 6H, Ar- $\text{CH}_3$ ), 2.11 (m, 2H), 1.65 (m, 8H, pyrrole- $\text{CH}_2\text{CH}_2$ ), 1.59 (m, 8H, pyrrole- $(\text{CH}_2)_2\text{CH}_2$ ), 1.32 (m, 12H, pyrrole- $(\text{CH}_2)_3\text{CH}_3$ ), 1.11 (m, 4H,  $\text{OCH}_2\text{CH}_2$ ), 0.92 (s, 9H,  $t\text{Bu}$ ), 0.37 (m, 4H,  $\text{O}(\text{CH}_2)_2\text{CH}_2$ ),  $-42$  (s, 1H, SH).

**12:** Carbon monoxide was bubbled through a solution of **10** in toluene for 3 h. A UV/Vis spectrum indicated the presence of the hexacoordinated CO complex **12**; UV/Vis ( $\text{CH}_2\text{Cl}_2$ ):  $\lambda_{\text{max}}$  (%) = 416 (100), 448 (27), 510 (8), 574 (5), 654 nm (2).

**7-DIMI:** To a solution of **7-Br $^-$**  (3 mg, 1.87  $\mu\text{mol}$ ) in MTHF (0.2 mL) was added **13** (18.4 mg, 0.191 mmol). The brown-red mixture was stirred at  $25^\circ\text{C}$  under argon for 24 h. After removal of solvent in vacuo, toluene (3 mL) was added, and the mixture was filtered over celite to remove the

excess of **13**. Subsequent evaporation of the solvents gave a brown solid; UV/Vis ( $\text{CH}_2\text{Cl}_2$ ):  $\lambda_{\text{max}}$  (%) = 402 (100), 512 (8), 592 nm (5).

**7-D<sub>2</sub>O and 7-H<sub>2</sub><sup>17</sup>O:** To a 10 mm solution of **7**-H<sub>2</sub>O (250  $\mu\text{L}$ ) in MTHF was added D<sub>2</sub>O (100  $\mu\text{L}$ ; Cambridge Isotope Laboratories, enrichment of D 99.996%) or H<sub>2</sub><sup>17</sup>O (100  $\mu\text{L}$ ; Cambridge Isotope Laboratories, enrichment of <sup>17</sup>O 46%), and the mixture was stirred at 25 °C under argon for 12 h. After removal of the water phase the solution was directly used for the EPR experiments.

**EPR and ENDOR sample preparation:** The solutions of **7**-H<sub>2</sub>O, **7**-D<sub>2</sub>O, **7**-H<sub>2</sub><sup>17</sup>O, and **7**-DIMI in MTHF (Fluka, purum), concentration 5–10 mM, were transferred to an EPR tube and degassed on a vacuum line by the freeze-pump-thaw method.

**EPR and ENDOR equipment:** The CW EPR spectra at 100 K were recorded on a Bruker ESP 300 spectrometer (microwave frequency 9.485 GHz) with use of a liquid nitrogen cryostat. The CW EPR spectra at 10 K and all pulse EPR and ENDOR spectra (3.3 K throughout) were recorded on a Bruker ESP 380 spectrometer (microwave frequency 9.717 GHz) with use of an Oxford liquid helium cryostat. The CW EPR spectra of frozen solutions were measured with a microwave power of 20 mW, a modulation amplitude of 0.5 mT, and a modulation frequency of 100 kHz. The magnetic field was measured with a Bruker NMR gaussmeter ER 035M. All pulse EPR and ENDOR measurements were conducted at a repetition rate of 1 kHz.

**Three-pulse ESEEM spectra:**<sup>[20]</sup> The experiments were carried out with the  $\pi/2$ - $\tau$ - $\pi/2$ - $t$ - $\pi/2$ - $\tau$ -echo pulse sequence, and a pulse length of 16 ns. The echo intensity was measured as a function of time  $t$ , which was incremented from 16 to 8200 ns in steps of 8 ns.  $\tau$  was varied between 88 and 592 ns in steps of 8 ns to avoid signal distortions due to blind spots. Four-step phase cycles were employed to eliminate unwanted echo contributions.<sup>[21]</sup>

**Davies ENDOR spectra:**<sup>[22]</sup> The spectra were recorded with the  $\pi$ - $t$ - $\pi/2$ - $\tau$ -echo pulse sequence, and a pulse length of 48 and 96 ns for the  $\pi/2$  and  $\pi$  pulses and a  $\tau$  value of 104 ns. A selective radio frequency (RF)  $\pi$  pulse of variable frequency  $\nu_{\text{RF}}$  was applied during the time interval  $t$ . The length of the RF pulse was 8504 ns, and the RF increment was set to 50 kHz.

**Manipulation of EPR and ENDOR data:** The data were processed with the program MATLAB 5.1. (The MathWorks, Inc., Natick, MA, USA). The time traces of the three-pulse ESEEM data were baseline corrected with a fifth-degree polynomial function and apodized with a Hamming window. Zero filling was performed prior to Fourier transformation. All frequency domain three-pulse ESEEM results represent absolute-value spectra. To remove blind spots, three-pulse ESEEM spectra measured at different  $\tau$  values were added together.

Received: June 2, 1998 [Z119321E]

German version: *Angew. Chem.* **1998**, *110*, 3191–3196

**Keywords:** cytochrome P450 • enzyme mimetics • EPR spectroscopy • porphyrinoids

- [1] P. Ortiz de Montellano, *Cytochrome P450. Structure, Mechanism, and Biochemistry*, 1st ed., Plenum, New York, **1986**; 2nd ed., Plenum, New York, **1995**.
- [2] a) T. L. Poulos, B. C. Finzel, I. C. Gunsalus, G. C. Wagner, J. Kraut, *J. Biol. Chem.* **1985**, *260*, 16122–16130; b) T. L. Poulos, B. C. Finzel, A. J. Howard, *Biochemistry* **1986**, *25*, 5314–5322.
- [3] a) T. L. Poulos, B. C. Finzel, A. J. Howard, *J. Mol. Biol.* **1987**, *195*, 687–700; b) R. Raag, T. L. Poulos, *Biochemistry* **1989**, *28*, 916–922; c) R. Raag, T. L. Poulos, *Biochemistry* **1989**, *28*, 7586–7592.
- [4] W.-D. Woggon, *Top. Curr. Chem.* **1996**, *184*, 39–96.
- [5] T. I. Oprea, G. Hummer, A. E. Garcia, *Proc. Natl. Acad. Sci. USA* **1997**, *94*, 2133–2138.
- [6] S. G. Sligar, *Biochemistry* **1976**, *15*, 5399–5406.
- [7] a) S. Shaik, M. Filatov, D. Schröder, H. Schwarz, *Chem. Eur. J.* **1998**, *4*, 193–199; b) M. Newcomb, M.-H. Le Tadic, D. A. Putt, P. F. Hollenberg, *J. Am. Chem. Soc.* **1995**, *117*, 3312–3313; c) M. Newcomb, M.-H. Le Tadic-Biadatti, D. L. Chestney, E. S. Roberts, P. F. Hollenberg, *J. Am. Chem. Soc.* **1995**, *117*, 12085–12091.
- [8] G. H. Loew, J. Collins, B. Luke, A. Waleh, A. Pudzianowski, *Enzyme* **1986**, *36*, 54–78.

- [9] a) H. Thomann, M. Bernardo, D. Goldfarb, P. M. H. Kroneck, V. Ullrich, *J. Am. Chem. Soc.* **1995**, *117*, 8243–8251; b) D. Goldfarb, M. Bernardo, H. Thomann, P. M. H. Kroneck, V. Ullrich, *J. Am. Chem. Soc.* **1996**, *118*, 2686–2693.
- [10] H. Aissaoui, S. Ghirlanda, C. Gmür, W.-D. Woggon, *J. Mol. Catal. A* **1996**, *113*, 393–402.
- [11] H. Aissaoui, W.-D. Woggon, unpublished results.
- [12] R. Tsai, C. A. Yu, I. C. Gunsalus, J. Peisach, W. Blumberg, W. H. Orme-Johnson, H. Beinert, *Proc. Natl. Acad. Sci. USA* **1970**, *66*, 1157–1163.
- [13] J. D. Lipscomb, *Biochemistry* **1980**, *19*, 3590–3599.
- [14] C. P. Scholes, A. Lapidot, R. Mascarenhas, T. Inubushi, R. A. Isaacson, G. Feher, *J. Am. Chem. Soc.* **1982**, *104*, 2724–2735.
- [15] a) R. Lohrutto, C. P. Scholes, G. C. Wagner, I. C. Gunsalus, P. G. Debrunner, *J. Am. Chem. Soc.* **1980**, *102*, 1167–1170; b) Y.-C. Fann, N. C. Gerber, P. A. Osmulski, L. P. Hager, S. G. Sligar, B. M. Hoffman, *J. Am. Chem. Soc.* **1994**, *116*, 5989–5990.
- [16] C. F. Mulks, C. P. Scholes, L. C. Dickinson, A. Lapidot, *J. Am. Chem. Soc.* **1979**, *101*, 1645–1654.
- [17] J. Peisach, W. B. Mims, J. L. Davis, *J. Biol. Chem.* **1984**, *259*, 2704–2706.
- [18] D. Harris, G. H. Loew, *J. Am. Chem. Soc.* **1993**, *115*, 8775–8779.
- [19] H. Aissaoui, R. Bachmann, A. Schweiger, W.-D. Woggon, unpublished results.
- [20] a) A. Schweiger, *Angew. Chem.* **1991**, *103*, 223–250; *Angew. Chem. Int. Ed. Engl.* **1991**, *30*, 265–292; b) S. A. Dikanov, Y. D. Tsvetkov, *Electron Spin Echo Envelope Modulation (ESEEM) Spectroscopy*, CRC, Boca Raton, FL, **1992**.
- [21] J.-M. Fauth, A. Schweiger, L. Braunschweiler, J. Forrer, R. R. Ernst, *J. Magn. Reson.* **1986**, *66*, 74–85.
- [22] E. R. Davies, *Phys. Lett. A* **1974**, *47A*, 1–2; b) C. Gemperle, A. Schweiger, *Chem. Rev.* **1991**, *91*, 1481–1505.

## Pyrrole Denitrogenation and Fragmentation of Tetramethylethylenediamine Promoted by a Nb<sup>II</sup> Cluster\*\*

Maryam Tayebani, Sandro Gambarotta,\* and Glenn P. A. Yap

In memory of Lucio Senatore

Metal-promoted cleavage of the C–N bond of amines is a very rare but desirable transformation. So far, this is limited to the cleavage of C–N bonds of strained amines<sup>[1]</sup> or amidines.<sup>[2]</sup> Only by using highly reactive trivalent Group 5 metals (Nb and Ta) was it possible to rupture the C–N single bond of aniline<sup>[3]</sup> and to afford ring-opening of the pyridine aromatic ring.<sup>[4]</sup> These remarkable reactions are important for the perspectives and the possibilities offered in terms of industrial applications such as denitrogenation<sup>[5]</sup> of crude oil, catalytic degradation of heterocycles,<sup>[6]</sup> catalysis, and extrusion of nitrogen and ammonia from organic compounds.<sup>[7]</sup>

We have recently described the serendipitous preparation and characterization of a Nb<sup>II</sup> cluster [(tmeda)<sub>2</sub>Nb<sub>2</sub>Cl<sub>3</sub>Li-

[\*] Prof. Dr. S. Gambarotta, M. Tayebani, Prof. G. P. A. Yap  
Department of Chemistry  
University of Ottawa  
Ottawa, Ontario, K1N 6N5 (Canada)  
Fax: (+1) 613-5672-5170  
E-mail: sgambaro@oreo.chem.uottawa.ca

[\*\*] This work was supported by the Natural Sciences and Engineering Council of Canada (NSERC) and by NATO (travel grant).